Host factors drive the within-host competition between highly and low pathogenic H5N8 avian influenza viruses

Pierre Bessière[1¶], Thomas Figueroa[1¶], Amelia Coggon[1], Charlotte Foret-Lucas[1], Alexandre Houffschmitt[1], Maxime Fusade-Boyer[1], Gabriel Dupré[1], Jean-Luc Guérin[1], Maxence Delverdier[1], and Romain Volmer[1*]

[1] Ecole nationale vétérinaire de Toulouse, Université de Toulouse, ENVT, INRAE, IHAP, UMR 1225, Toulouse, France.

* Correspondence:

Dr Romain Volmer

romain.volmer@envt.fr

¶ These authors contributed equally to this work.

ABSTRACT

Highly pathogenic avian influenza viruses (HPAIV) emerge from low pathogenic avian influenza viruses (LPAIV) through the introduction of basic amino acids at the hemagglutinin (HA) cleavage site. Following viral evolution, the newly formed HPAIV likely represents a minority variant within the index host, predominantly infected with the LPAIV precursor. Using reverse-genetics engineered H5N8 viruses differing solely at the HA cleavage, we tested the hypothesis that the interaction between the minority HPAIV and the majority LPAIV could modulate the risk of HPAIV emergence and that the nature of the interaction could depend on the host species. In chickens, we observed that the $H5N8_{LP}$ increased $H5N8_{HP}$ replication and pathogenesis. By contrast, the $H5N8_{LP}$ antagonized $H5N8_{HP}$ replication and pathogenesis in ducks. Ducks mounted a more potent antiviral innate immune response than chickens against the $H5N8_{LP}$, which correlated with $H5N8_{HP}$ inhibition. These data provide experimental evidence that HPAIV may be more likely to emerge in chickens than in ducks and underscore the importance of within-host viral variants interactions in viral evolution.

34 **INTRODUCTION**

35 Highly pathogenic avian influenza virus (HPAIV) outbreaks have a major
36 impact on animal health, food security and economy, as well as on public
37 health (EFSA Panel on Animal Health and Welfare (AHAW) et al., 2017; Lee
38 et al., 2021). A better understanding of the factors leading to HPAIV
39 emergence is therefore of paramount importance. Avian influenza viruses
40 of H5 and H7 subtypes can become highly pathogenic through the
41 introduction of multiple basic amino acids within the hemagglutinin (HA)
42 cleavage site (Böttcher-Friebertshäuser et al., 2014). Several mechanisms
43 account for these introductions: nucleotide substitutions and insertions or
44 non-homologous recombination with viral or cellular RNAs (Abdelwhab et
45 al., 2013; Lee et al., 2021; Richard et al., 2017). The acquisition of a multi-
46 basic cleavage site (MBCS) is a virus-dependent event that occurs in a bird
47 infected with a parental low pathogenic avian influenza virus (LPAIV). To
48 emerge successfully, the newly formed HPAIV must become a predominant
49 variant in order to overcome the transmission bottleneck between
50 individuals (Hughes et al., 2012; McCrone and Lauring, 2018; Varble et al.,
51 2014). In order to achieve this, the newly formed HPAIV must therefore
52 outcompete its LPAIV precursor within the individual in which it has
53 arisen. We therefore suggest that HPAIV emergence is a two-step process:
54 firstly, the acquisition of a MBCS, followed by the ability to become a
55 predominant variant of the viral quasi-species within an individual.
56 Over the past decades, the vast majority of HPAIV emergences have been
57 linked to H5 and H7 LPAIV circulation in *Galliformes* (such as chickens and
58 turkeys) (Abdelwhab et al., 2013; EFSA Panel on Animal Health and
59 Welfare (AHAW) et al., 2017; Lee et al., 2021). By contrast, *Anseriformes*
60 (such as ducks and geese) are considered as reservoirs for LPAIV
61 precursors, rather than a species in which HPAIV emerge (Bodewes and
62 Kuiken, 2018; Munster et al., 2007; van Dijk et al., 2018; Wahlgren, 2011).
63 These observations suggest that host factors could modulate HPAIV
64 emergence. To our knowledge, this has never been investigated
65 experimentally.

66 To model the intra-host competition between a newly formed HPAIV and
67 its parental LPAIV, we co-infected embryonated eggs and chickens and
68 ducks *in vivo* with a H5N8 HPAIV as a minority variant and a reverse-
69 genetics engineered LPAIV that differed from the HPAIV only at the level of
70 the HA cleavage site, as a majority variant. Our results demonstrate that
71 chickens and ducks have opposite effects on the interaction between the
72 H5N8 HPAIV and LPAIV and that the HPAIV has a stronger selective
73 advantage in chickens than in ducks. To our knowledge this is the first
74 experimental evidence that HPAIV emergence could be more likely in
75 chickens than in ducks.

76

77 **RESULTS**

78 **Characterization of $H5N8_{HP}$ and $H5N8_{LP}$ viruses in cell culture**

79 We used reverse-genetics to generate the wild-type $H5N8_{HP}$ from a HPAIV
80 isolated during the 2016 H5N8 epizootics in France (Guinat et al., 2018).
81 This virus belonged to clade 2.3.4.4 group B, which caused high levels of
82 mortality in *Galliformes* and in wild and domestic *Anseriformes* during the
83 2016-2017 HPAIV outbreak in Europe (Grund et al., 2018; Guinat et al.,
84 2018; Kleyheeg et al., 2017; More et al., 2017). Using site-directed
85 mutagenesis and reverse-genetics, we mutated the $H5N8_{HP}$ HA polybasic
86 cleavage site PLRELRRLR/G to a monobasic cleavage site PQRETR/G to
87 obtain the $H5N8_{LP}$ virus with a typical LPAIV HA sequence (NCBI Genbank
88 accession number: AB261853.1) (Hiono et al., 2016). The $H5N8_{HP}$ and the
89 $H5N8_{LP}$ differed solely at the level of the HA cleavage site, as verified by
90 whole genome sequencing following virus amplification in chicken
91 embryonated eggs (Fig. 1A).
92 Viral growth kinetics was analyzed in Madin-Darby canine kidney (MDCK)
93 cells, in the DF-1 chicken fibroblast cell line and in the CCL-141 duck
94 fibroblast cell line infected at a multiplicity of infection (MOI) of 10^{-5} tissue
95 culture infectious dose 50 ($TCID_{50}$). $H5N8_{HP}$ replicated with similar kinetics
96 in the absence or presence of exogenous trypsin, demonstrating that
97 proteolytic processing of the HA MBCS was independent of trypsin-like

98 proteases, as expected for a HPAIV (Fig. 1B). By contrast, $H5N8_{LP}$
99 replication was severely impaired in the absence of trypsin, while its
100 replication kinetics was indistinguishable from that of the $H5N8_{HP}$ in the
101 presence of trypsin (Fig. 1B). These results indicate that mutations
102 introduced in the $H5N8_{LP}$ HA have no negative impact on viral replication
103 kinetics in cell culture beyond the expected trypsin-like proteases
104 requirement for $H5N8_{LP}$ HA proteolytic processing, as expected for a LPAIV.
105

106 **$H5N8_{HP}$ and $H5N8_{LP}$ viruses co-infections *in ovo***

107 Next, we evaluated $H5N8_{HP}$ and $H5N8_{LP}$ replication in embryonated chicken
108 (*Gallus gallus*) and Pekin duck (*Anas platyrhynchos domesticus*) eggs, as
109 they have a complex cellular architecture and provide an intermediate
110 model between monolayer cell culture and *in vivo* studies. To investigate
111 how the host species modulated the interaction between a HPAIV and a
112 LPAIV, we inoculated embryonated chicken and duck eggs via the allantoic
113 cavity either with 10^2 egg infectious dose 50 (EID_{50}) $H5N8_{HP}$ alone, with
114 increasing doses of $H5N8_{LP}$ alone, or with 10^2 EID_{50} $H5N8_{HP}$ in combination
115 with increasing doses of $H5N8_{LP}$ (Fig. 2A). We inoculated chicken eggs at
116 day 10 and duck eggs at day 11 in order to work at similar development
117 stages (Li et al., 2019). After 24 hours of incubation at 37°C, we harvested
118 the allantoic fluid and quantified the level of virus replication by RT-qPCR
119 using primers specific for $H5N8_{HP}$ or $H5N8_{LP}$ HA. In chicken eggs, we
120 detected equivalent levels of viral RNA following inoculation with 10^2EID_{50}
121 $H5N8_{HP}$ alone or with $H5N8_{LP}$ alone regardless of the inoculum dose (Fig.
122 2B). Upon co-infection with $H5N8_{HP}$ and $H5N8_{LP}$ in chicken eggs, the level
123 of $H5N8_{HP}$ and $H5N8_{LP}$-specific viral RNA did not differ from mono-
124 infections regardless of the quantity of $H5N8_{LP}$ (Fig. 2B). Thus, the
125 replication of $H5N8_{HP}$ is not affected by $H5N8_{LP}$, regardless of the amount of
126 $H5N8_{LP}$ co-inoculated in chicken eggs. In duck eggs, we detected similar
127 levels of viral RNA following inoculation with 10^2 EID_{50} $H5N8_{HP}$ alone or
128 with 10^2 EID_{50} $H5N8_{LP}$ alone (Fig. 2C). When duck eggs were infected
129 simultaneously with $H5N8_{HP}$ and $H5N8_{LP}$, we observed a decrease of
130 $H5N8_{HP}$ viral RNA levels that correlated with the amount of $H5N8_{LP}$ co-

131 inoculated, indicating that the $H5N8_{LP}$ antagonized $H5N8_{HP}$ replication in
132 duck eggs (Fig. 2C). The *in ovo* experiments provide evidence that a ≥100-
133 fold excess of $H5N8_{LP}$ significantly antagonized $H5N8_{HP}$ replication in duck
134 eggs, while $H5N8_{LP}$ did not affect $H5N8_{HP}$ replication in chicken eggs
135 regardless of the amount of $H5N8_{LP}$. This observation thus indicates that
136 the $H5N8_{HP}$ had a stronger selective advantage over the $H5N8_{LP}$ in chicken
137 embryonated eggs than in duck embryonated eggs.
138

139 **Potentiation of HPAIV replication and pathogenesis by LPAIV in**
140 **chickens**

141 In a preliminary experiment (data not shown), we observed transient low-
142 level oropharyngeal viral RNA shedding in 6/8 of the 10^6 EID_{50} $H5N8_{LP}$
143 infected chickens (*Gallus gallus*), whereas all chickens infected with 10^7
144 EID_{50} $H5N8_{LP}$ shed high levels of viral RNA for a prolonged time. No clinical
145 signs were observed in chickens inoculated with $H5N8_{LP}$. Furthermore, by
146 using increasing doses of $H5N8_{HP}$, we evaluated the $H5N8_{HP}$ chicken
147 infectious dose 50 at $6x10^3$ EID_{50} and noticed that mortality reached 100%
148 within four days with doses higher than 10^5 EID_{50}. $H5N8_{HP}$-infected sick
149 birds presented dyspnea that quickly progressed to severe dyspnea,
150 associated with anorexia and lethargy. These results provided evidence
151 that the $H5N8_{HP}$ and $H5N8_{LP}$ caused, respectively, commonly observed
152 HPAIV and LPAIV-associated infection patterns in chickens (EFSA Panel on
153 Animal Health and Welfare (AHAW) et al., 2017).
154 Based on these results, we investigated the interaction between a HPAIV
155 and a LPAIV in chickens. Four-week old chickens were assigned one of six
156 groups: L7, H3, H4, L7H3, L7H4 or NI (Fig. 3A). L7 animals were infected
157 with 10^7 EID_{50} $H5N8_{LP}$. H3 animals were infected with 10^3 EID_{50} $H5N8_{HP}$.
158 H4 animals were infected with 10^4 EID_{50} $H5N8_{HP}$. L7H3 animals were
159 infected with a mixture of 10^7 EID_{50} $H5N8_{LP}$ and 10^3 EID_{50} $H5N8_{HP}$. L7H4
160 animals were infected with a mixture of 10^7 EID_{50} $H5N8_{LP}$ and 10^4 EID_{50}
161 $H5N8_{HP}$. Finally, non-infected animals from group NI were administered
162 vehicle only. Neither mortality nor clinical signs were observed in chickens
163 from group L7 and group H3 (Fig. 3B). Chickens in the H4 group reached

164 45% mortality (Fig. 3B). When chickens were infected with a mixture of
165 $H5N8_{LP}$ and $H5N8_{HP}$, we observed an increase in mortality compared to
166 $H5N8_{HP}$ mono-infected chickens: mortality reached 18% in the L7H3 group,
167 compared to 0% in the H3 group; and 72% in the L7H4 group, compared to
168 45% in the H4 group (Fig. 3B). Although the increase in mortality did not
169 reach statistical significance, these results indicate that $H5N8_{LP}$ and $H5N8_{HP}$
170 synergized, resulting in increased pathogenesis in co-infected chickens
171 compared to $H5N8_{HP}$ mono-infected chickens.
172 We measured viral shedding from oropharyngeal and cloacal swabs by
173 quantifying viral RNA using RT-qPCR with primers detecting specifically
174 $H5N8_{LP}$ or $H5N8_{HP}$ HA sequences. Regardless of the experimental group, all
175 $H5N8_{HP}$ swab-positive chickens eventually developed severe dyspnea and
176 either died or were euthanized when they reached humane endpoints, as
177 previously observed (Leyson et al., 2019). In line with the mortality rate
178 (Fig 3B), no $H5N8_{HP}$ swab-positive chicken was found in the H3 group,
179 while only two chickens tested positive for $H5N8_{HP}$ in the L7H3 group.
180 Because of the low rate of infection in the H3 and L7H3 groups, these
181 animals were excluded from further analyses. $H5N8_{HP}$ oropharyngeal and
182 cloacal shedding was higher in group L7H4 compared to group H4 at 2 days
183 post-infection (dpi), but the difference was not statistically significant (Fig.
184 3C&D). Average $H5N8_{HP}$ oropharyngeal and cloacal shedding remained
185 otherwise similar between the L7H4 and the H4 groups and was not
186 associated with different $H5N8_{HP}$ transmission rates to contact chickens
187 introduced in the poultry isolators at 1 dpi (data not shown). $H5N8_{LP}$
188 oropharyngeal shedding did not differ between the L7 and L7H4 group
189 (Fig. 3E).

190 **Antagonism of HPAIV replication and pathogenesis by LPAIV in ducks**

191 We inoculated groups of 4-week old Pekin ducks (*Anas platyrhynchos*
192 *domesticus*) with $H5N8_{HP}$ alone, $H5N8_{LP}$ alone, or a mixture containing both
193 $H5N8_{LP}$ and $H5N8_{HP}$. Ducks were assigned one of four groups: L7, H4, L7H4
194 or NI (Fig. 7A). L7 animals were infected with 10^7 EID_{50} $H5N8_{LP}$. H4 animals
195 were infected with 10^4 EID_{50} $H5N8_{HP}$. L7H4 animals were infected with a
196 mixture of 10^7 EID_{50} $H5N8_{LP}$ and 10^4 EID_{50} $H5N8_{HP}$. Non-infected animals

197 from group NI were administered vehicle only. Neither mortality nor
198 clinical signs were observed in any duck of group L7 (Fig. 7B). Mortality
199 reached 87% in the H4 group and was preceded by predominantly
200 neurological clinical signs, in accordance with the pronounced
201 neurotropism of clade 2.3.4.4 group B H5N8 viruses in ducks (Grund et al.,
202 2018; Kleyheeg et al., 2017; More et al., 2017). Mortality was significantly
203 reduced to 37% in the L7H4 group. Thus, $H5N8_{LP}$ antagonized $H5N8_{HP}$
204 pathogenesis in co-infected ducks, in contrast to what we observed in
205 chickens.
206 To determine how this related to the levels of virus replication, we
207 analyzed $H5N8_{LP}$ and $H5N8_{HP}$ viral RNA shedding from oropharyngeal and
208 cloacal swabs using RT-qPCR. Oropharyngeal $H5N8_{HP}$ shedding was
209 significantly reduced in group L7H4 compared to group H4 in the first days
210 post-infection (dpi), with a hundred-fold difference at 1 dpi ($p<0.001$) and
211 a ten-fold difference at 2 and 3 dpi ($p<0.01$) (Fig. 7C). Cloacal $H5N8_{HP}$
212 shedding was also decreased in group L7H4, but the difference only
213 reached statistical difference at day 3, with a ten-fold reduction ($p<0.05$)
214 (Fig. 7D). There was no difference in $H5N8_{LP}$ shedding between groups
215 L7H4 and L7 (Fig. 7E).
216 Next, we analyzed viral RNA levels in the lungs and brain. $H5N8_{LP}$ was not
217 detected in the lungs or brain, indicating that $H5N8_{LP}$ replicated mostly in
218 the upper respiratory tract of ducks. In contrast to chickens, we detected
219 $H5N8_{HP}$ nucleic viral RNA from the lungs and brain of most animals at 1 and
220 3 dpi (Fig. 7F&G). $H5N8_{HP}$ viral RNA load was decreased in the lungs and
221 brain of $H5N8_{LP}$ and $H5N8_{HP}$ co-infected birds (group L7H4), compared to
222 $H5N8_{HP}$ mono-infected birds (group H4). High levels of $H5N8_{HP}$ viral RNA
223 were also detected in the lungs and brain of moribund ducks, which
224 developed predominantly neurological signs.
225 Extensive viral antigen staining was detected by immunohistochemistry in
226 the brain of moribund animals, while more modest viral antigen staining
227 was observed in the lungs, with no difference between groups L7H4 and H4
228 (Fig. 8A&B). We then evaluated the expression of host immune response
229 markers in the lungs and brain using RT-qPCR. Mx mRNA expression was

230 significantly increased in the lungs of infected ducks belonging to the L7H4
231 and H4 groups at 1 and 3 dpi, as well as in moribund animals (Fig. 9A).
232 Compared to NI duck, we also observed an upregulation of Mx mRNA
233 expression in the lungs of $H5N8_{LP}$ mono-infected ducks (L7 group) at 1 and
234 3 dpi, although the difference did not reach statistical significance. IFN-γ
235 mRNAs levels were significantly higher in the lungs of $H5N8_{HP}$ mono-
236 infected ducks (group H4) at 1 dpi compared to NI, L7H4 and L7 ducks (Fig.
237 9B). Similar results were observed in the brain (data not shown). To
238 evaluate the antiviral innate immune response in the upper respiratory
239 tract, we measured Mx mRNA expression by RT-qPCR from RNA extracted
240 from oropharyngeal swabs. Compared to NI ducks, Mx mRNA was
241 increased in all infected groups (Fig. 9C). In contrast to chickens, Mx mRNA
242 expression level remained high in $H5N8_{LP}$ mono-infected ducks from the L7
243 group (Fig. 9C).

244 To further compare the antiviral innate immune response in ducks and
245 chickens, we plotted the levels of Mx mRNA as a function of the level of viral
246 RNA in the lungs (Fig. 10A). We observed a correlation between the level of
247 Mx mRNA and the level of viral RNA in ducks (Pearson $r=0.64$; $p<0.001$),
248 confirming that the intensity of the antiviral innate immune response is
249 proportional to the level of viral RNA, as previously reported (Baccam et al.,
250 2006; Hagenaars et al., 2016; Soubies et al., 2013; Volmer et al., 2011). This
251 correlation was less visible in chickens, possibly because viral RNA was
252 only found in the lungs of a limited number of chickens (Pearson $r=0.50$;
253 $p=0.21$). The Mx/HA ratios were distributed to higher values in ducks
254 compared to chickens (Fig. 10A), resulting in mean Mx/HA ratios that were
255 significantly higher in ducks than in chickens (Fig. 10B). This result
256 demonstrates that ducks mounted a more potent antiviral innate immune
257 response against influenza virus infection than chickens.
258

259 **DISCUSSION**

260 To model the intra-host competition between a newly formed HPAIV and
261 its parental LPAIV, we inoculated chickens and ducks with an $H5N8_{HP}$ virus
262 and an $H5N8_{LP}$ virus differing solely at the level of the HA cleavage site.
263 When inoculated alone, $H5N8_{HP}$ replication and pathogenesis were
264 equivalent in chickens and ducks. However, when chickens and ducks were
265 co-inoculated with this pair of viruses, we found that the $H5N8_{HP}$ had a
266 stronger selective advantage over the $H5N8_{LP}$ in chickens than in ducks.
267 Surprisingly, we observed that the $H5N8_{LP}$ increased $H5N8_{HP}$ replication
268 and pathogenesis in chickens. By contrast, we observed that the $H5N8_{LP}$
269 antagonized $H5N8_{HP}$ replication and pathogenesis in ducks. Thus, the
270 nature of the interaction between the HPAIV and the parental LPAIV may
271 be a critical determinant of HPAIV emergence, which we show here to
272 depend on the host species.

273 The interaction between co-infecting viruses ranges from synergy to
274 antagonism depending on the virus pairs and the host (Andreu-Moreno et
275 al., 2020; Bou et al., 2019; DaPalma et al., 2010; Domingo-Calap et al., 2019;
276 Kumar et al., 2018; Opatowski et al., 2018; Phipps et al., 2020). Functional
277 complementation occurs when one virus provides a function that is absent
278 or less efficient in the other virus. As the genomes of the $H5N8_{HP}$ and
279 $H5N8_{LP}$ differ solely at the level of the HA cleavage site, it is unlikely that
280 the $H5N8_{LP}$ is able to provide a function missing in the $H5N8_{HP}$. We
281 therefore speculate that the $H5N8_{LP}$-mediated increase in $H5N8_{HP}$
282 replication and pathogenesis observed in chickens could be due to
283 complementation of semi-infectious $H5N8_{HP}$ particles by the $H5N8_{LP}$
284 inoculated at a higher dosage (Brooke, 2017). Such complementation is
285 likely to occur both in chickens and in ducks. However, this
286 complementation may be undetectable in ducks due to the dominant effect
287 of host-mediated antagonism between the $H5N8_{LP}$ and the $H5N8_{HP}$. The
288 antagonism between the $H5N8_{LP}$ and the $H5N8_{HP}$ is unlikely to be due to
289 viral interference due to receptor or cell machinery usage, as no
290 competition between the $H5N8_{LP}$ and the $H5N8_{HP}$ was observed in

291 chickens, although the $H5N8_{LP}$ replicated to higher levels and persisted
292 longer in chickens than in ducks. In contrast to chickens, ducks have a
293 functional RIG-I receptor, which has been proposed to contribute to the
294 more efficient type I interferon mediated-antiviral innate immune response
295 against influenza viruses observed in ducks compared to chickens (Barber
296 et al., 2010; Burggraaf et al., 2014; Cornelissen et al., 2013, 2012; Kuchipudi
297 et al., 2014; Magor et al., 2013; Soubies et al., 2013). The $H5N8_{LP}$ and the
298 $H5N8_{HP}$ are likely to be intrinsically equally sensitive to the antiviral effects
299 of type I interferon. However, a stronger antiviral innate immune response
300 could impose a stronger selective pressure on the minority variant (Zwart
301 and Elena, 2015). In line with this hypothesis, type I interferon antiviral
302 innate immune response was shown to constitute a strong bottleneck
303 shaping poliovirus population in mice (Kuss et al., 2008). Similarly,
304 treatment of hepatitis C virus-infected patients with type I IFN resulted in a
305 dramatic reduction of viral diversity (Farci et al., 2002). Furthermore, a
306 delayed type I IFN response in influenza A virus-infected obese mice
307 promoted minority variant emergence, while type I interferon treatment
308 reduced viral diversity (Honce et al., 2020). Altogether, these results
309 indicate that the innate immunity can shape viral populations. By
310 decreasing viral replication and increasing the within-host competition
311 between variants, a strong innate immune response may inhibit the
312 selection of variants that arise through *de novo* mutations during infection
313 of an individual, unless these variants have a strong selective advantage
314 within this individual. We suggest that the more pronounced antiviral
315 innate immune response observed in ducks compared to chickens may
316 impact the $H5N8_{HP}$ minority variant more severely in ducks than in
317 chickens. Admittedly, the differential outcome of $H5N8_{HP}$ and $H5N8_{LP}$ co-
318 infections in chickens and ducks may also depend on other host factors,
319 including microbiota composition or receptor distribution (Figueroa et al.,
320 2020; Hiono et al., 2016).

321 Recent work investigating the interaction between an H7N7 HPAIV and a
322 closely related H7N7 LPAIV field isolate demonstrated that the LPAIV
323 inhibited HPAIV replication in chickens when the LPAIV was inoculated at a

≥ 100-fold higher dose (Graaf et al., 2018). These results indicate that the nature of the interaction between the HPAIV and the LPAIV may depend on the viral strain. If competition between a LPAIV and a HPAIV occurred in chickens, we speculate that the competition could even be stronger in ducks, because of the stronger antiviral innate immune-mediated selective pressure imposed on the minority HPAIV. However, further work is needed to properly address this question. These studies should ideally be performed using different pairs of reverse-genetics engineered HPAIV and LPAIV differing solely at the level of the HA cleavage site to specifically investigate how the selective advantage conferred by the MBCS depends on the host species.

Epidemiological investigations of HPAIV outbreaks indicate that the vast majority of HPAIV emerge upon replication and inter-individual transmission of a LPAIV in *Galliformes*, such as chickens and turkeys, although *Anseriformes*, such as ducks and geese, are considered as the main reservoirs for LPAIV (Abdelwhab et al., 2013; EFSA Panel on Animal Health and Welfare (AHAW) et al., 2017; Lee et al., 2021; Richard et al., 2017). In this study, we focused on the two main representatives of the *Galliformes* and *Anseriformes* orders: chickens, which are with current global production of 22 billion chickens the main source of animal protein for human consumption worldwide and Pekin ducks, which are also intensively raised in farms and represent the best characterized *Anseriformes* in respect to the interaction with influenza viruses (Lee et al., 2021; "Poultry species | Gateway to poultry production and products | Food and Agriculture Organization of the United Nations," n.d.). How the LPAIV and the newly formed HPAIV would interact in other bird species, such as turkeys, or in wild dabbling or diving ducks, which have a prominent role in the ecology of avian influenza viruses will be the subject of future studies (Bodewes and Kuiken, 2018; EFSA Panel on Animal Health and Welfare (AHAW) et al., 2017; Lee et al., 2021). In addition to host factors, anthropic factors are also likely to play a major role in the emergence of HPAIV and may contribute to the higher frequency of HPAIV emergence observed in chickens that are usually raised at higher densities than ducks (Capua and

357 Marangon, 2000; Dhingra et al., 2018; M.c et al., 2009; Richard et al., 2017).
358 Estimating to which extent farming processes contribute to the emergence
359 of HPAIV is however a difficult task and therefore their contribution to
360 HPAIV emergence remains currently unclear.

361 To minimize the risk of HPAIV evolution, present European regulation and
362 national regulations in many countries require the culling of all birds in
363 flocks infected with H5 and H7 LPAIV (EFSA Panel on Animal Health and
364 Welfare (AHAW) et al., 2017). Culling of H5 or H7 LPAIV infected flocks
365 aims at eliminating LPAIV from the susceptible poultry population before
366 they have a chance to evolve into HPAIV, and is therefore considered a
367 preventive biosecurity measure. However, the broader public, breeders and
368 professional breeder societies question the need for preventive culling for
369 economical, animal welfare and breeder welfare issues (Organization,
370 2008). Indeed, preventive culling of animals, especially healthy animals,
371 which is commonly the case in LPAIV infected *Anseriformes*, is poorly
372 accepted. Identifying how host factors modulate HPAIV emergence
373 therefore provides important scientific data that may be taken into account
374 by animal health policy makers in the future.

375 ## MATERIALS AND METHODS

376 ### Viruses

377 The eight segments from the HPAIV field isolate A/mulard
378 duck/France/171201g/2017 (H5N8) were cloned in a pHW2000 plasmid
379 vector using a set of universal primers in order to generate a reverse-
380 genetics engineered wild-type HPAIV H5N8 ($H5N8_{HP}$) (Hoffmann et al.,
381 2001, 2000). Using site-directed mutagenesis, a 9 nucleotides deletion was
382 performed on the HA cleavage site sequence, along with two single
383 nucleotide polymorphism on both sides of the deletion to obtain a reverse-
384 genetics engineered LPAIV H5N8 ($H5N8_{LP}$) according to the manufacturer's
385 instructions (In-Fusion, Takara Bio, France). $2.5x10^5$ HEK 293T cells
386 cultured in 6-well plates were transfected in Opti-MEM medium, using the
387 lipophilic transfection reagent LTX with Plus reagent (Invitrogen, Thermo
388 Fisher Scientific Inc., Canada), either with 0.5µg of each seven common
389 $H5N8_{HP/LP}$ pHW2000 plasmids (PB2, PB1, PA, NA, NP, M and NS) and with
390 0.5µg of HA_{HP} or HA_{LP}. L-(tosylamido-2-phenyl)ethyl chloromethyl ketone
391 (TPCK) treated trypsin (TPCK-treated) was added 24 hours post-
392 transfection at a 0.5µg/ml final concentration. 48 hours post-transfection,
393 scraped cells and culture medium were transferred on MDCK cells grown
394 with Opti-MEM supplemented with 0.5µg/ml TPCK-treated trypsin. 72
395 hours later, cell supernatant was collected. To produce viral stock, both
396 viruses were then propagated in 10-day-old chicken specific-pathogen-free
397 (SPF) embryonated chicken eggs (INRAE, PFIE, Nouzilly, France), by
398 inoculation in the allantoic cavity of 100µL of 1:100 dilutions of infected
399 MDCK cells supernatant. Infectious allantoic fluid was harvested at 72
400 hours postinoculation and titrated in 10-day-old SPF embryonated chicken
401 eggs to determine the 50% egg infective dose (EID_{50})/mL using the Reed-
402 Muench method. The identity of amplified viruses was verified by Sanger
403 sequencing of each viral gene segment ($H5N8_{HP}$: accession numbers
404 MK859904 to MK859911; $H5N8_{LP}$: accession numbers MK859926 to
405 MK859933). These viruses were referenced by the French biotechnology
406 ethics committee (Haut Conseil des Biotechnologies) and were manipulated
407 exclusively in biosafety level 3 laboratories.

408

409 ***In vitro* infections**

410 MDCK cells, DF-1 cells and CCL-141 cells were cultured in DMEM
411 containing 1% antibiotics (penicillin/streptomycin) and 10% fetal bovine
412 serum. When cells reach 90% confluency, they were washed with PBS and
413 infected either with $H5N8_{HP}$ or with $H5N8_{LP}$ at a multiplicity of infection
414 (MOI) of 10^{-5} $TCID_{50}$. After one hour, the inoculum was removed, cells were
415 washed twice with PBS and Opti-MEM supplemented with 0.5µg/mL TPCK-
416 treated trypsin (Pierce, Thermo Fisher Scientific Inc., Canada) was added.
417 Viral RNA extraction was performed on 140µL supernatant collected at 1,
418 24, 48 and 72 hours post-infection according to the manufacturer's
419 instructions (QIAamp viral RNA; Qiagen, Toronto, Canada). Influenza
420 nucleic acid load was determined by RT-qPCR using primers targeting both
421 $H5N8_{LP}$ and $H5N8_{HP}$ HA gene in a final volume of 10µL. Mixes were
422 prepared according to the manufacturer's instructions (iTaq Universal
423 SYBR green One-Step kit, BioRad) with 1µL of RNA and a final
424 concentration of 0.3µM of each primer.

425

426 ***In ovo* co-infection experiments**

427 Specific pathogen-free (SPF) White Leghorn (PA12) embryonated chicken
428 eggs (PFIE, INRAE, Nouzilly, France) and Pekin Duck (ST5 Heavy)
429 embryonated eggs (ORVIA-Couvoir de la Seigneurtière, Vieillevigne,
430 France) were respectively incubated for 10 and 11 days at 37°C to work at
431 similar stages of development (Li et al., 2019). They were then inoculated
432 in the allantoic cavity with 200µL virus diluted in PBS containing 1%
433 antibiotics (penicillin/streptomycin). Eggs from group H2 were infected
434 with 10^2 EID_{50} $H5N8_{HP}$. Eggs from groups L2, L3, L4 and L5 were infected
435 with 10^2 EID_{50}, 10^3 EID_{50}, 10^4 EID_{50}, and 10^5 EID_{50} $H5N8_{LP}$ respectively. Eggs
436 from groups L2H2, L3H2, L4H2 and L5H2 were infected with a mixture of
437 10^2 EID_{50} $H5N8_{HP}$ and increasing doses of $H5N8_{LP}$: 10^2, 10^3, 10^4 and 10^5
438 EID_{50} $H5N8_{LP}$ respectively. Each group contained 9 to 29 eggs from two to
439 three independent experiments. 24 hours post-infection eggs were

440 incubated at 4°C overnight and allantoic fluid was harvested for RNA
441 extraction.

442

443 **Animals and groups**

444 Chickens and ducks experiment were conducted separately. One-day-old
445 Pekin ducklings (*Anas platyrhyncos domesticus*, ST5 heavy) were obtained
446 from a commercial hatchery (ORVIA-Couvoir de la Seigneurtière,
447 Vieillevigne, France) and one-day-old White Leghorn chicks (*Gallus gallus*
448 *domesticus*, PA12) from a research hatchery (PFIE, INRAE, Nouzilly,
449 France). Animals were fed *ad libitum* with a starter diet and housed in
450 biosafety level II facilities for 2 weeks in a litter-covered floor pen at the
451 National Veterinary School of Toulouse, France. They were then transferred
452 into a biosafety level III facility, equipped with bird isolators (I-Box; Noroit,
453 Nantes, France) ventilated under negative pressure with HEPA-filtered air.
454 Chicken preliminary experiment: 39 chickens were randomly assigned to
455 four groups: 10 animals were assigned to group H3 and were infected with
456 10^3 EID_{50} $H5N8_{HP}$. 10 animals were assigned to group H4 and were infected
457 with 10^4 EID_{50} $H5N8_{HP}$. 8 animals were assigned to group L6 and were
458 infected with 10^6 EID_{50} $H5N8_{LP}$. 11 animals were assigned to group L7 and
459 were infected with 10^7 EID_{50} $H5N8_{LP}$.
460 Chickens co-infection experiment: A total of 130 chickens were randomly
461 assigned to 4 groups: 26 animals (including 5 contact birds introduced 24
462 hours post-infection) were assigned to group H3 and were infected with
463 10^3 EID_{50} $H5N8_{HP}$. 26 animals (including 5 contact birds) were assigned to
464 group H4 and were infected with 10^4 EID_{50} $H5N8_{HP}$. 21 animals were
465 assigned to group L7 and were infected with 10^7 EID_{50} $H5N8_{LP}$. 26 animals
466 (including 5 contact birds) were assigned to group L7H3 and were
467 simultaneously infected with a mixture of 10^7 EID_{50} $H5N8_{LP}$ and 10^3 EID_{50}
468 $H5N8_{HP}$. 26 animals (including 5 contact birds) were assigned to group
469 L7H4 and were simultaneously infected with a mixture of 10^7 EID_{50} $H5N8_{LP}$
470 and 10^4 EID_{50} $H5N8_{HP}$. 5 animals were assigned to the non-infected control
471 group (NI).

472 Ducks co-infection experiment: A total of 64 ducks were randomly assigned
473 to 4 groups: 21 animals (including 3 contact birds) were assigned to group
474 H4 and were infected with 10^4 EID_{50} $H5N8_{HP}$. 16 animals were assigned to
475 group L7 and were infected with 10^7 EID_{50} $H5N8_{LP}$. 21 animals (including 3
476 contact birds) were assigned to group L7H4 and were simultaneously
477 infected with a mixture of 10^7 EID_{50} $H5N8_{LP}$ and 10^4 EID_{50} $H5N8_{HP}$. 5
478 animals were assigned to the non-infected control group (NI).
479
480 ***In vivo* experimental infections**
481 Serum was collected from all animals pre-infection to ensure that they
482 were serologically negative to influenza virus by using a commercial
483 influenza A NP antibody competition enzyme-linked immunosorbent assay
484 kit (ID Screen; ID-Vet, Montpellier, France) according to the manufacturer's
485 instructions. When they were 4-week-old, animals were infected through
486 the choanal route using an inoculum volume of 100µL. Non-infected groups
487 received the equivalent volume of allantoic fluid collected from non-
488 infected SPF embryonated chicken eggs. Contact birds were introduced in
489 the poultry isolators 1 day post-infection. Clinical signs were recorded over
490 8 to 9 days. Oropharyngeal and cloacal swabs were performed on all
491 animals daily. 5 animals from each group were humanely euthanized and
492 necropsied at 1 and 3 dpi. Moribund animals reaching humane termination
493 criteria (as dyspnea, convulsions, severe lethargy) were humanely killed
494 and also necropsied. For each necropsied animal, brain and lungs were
495 collected and stored frozen in TRIzol reagent (Invitrogen, Carlsbad, CA) or
496 stored in 10% neutral formalin.
497
498 **$H5N8_{LP}$ and $H5N8_{HP}$ quantification**
499 Cloacal and oropharyngeal swabs from *in vivo* experiments were briefly
500 vortexed in 500µL of sterile PBS and viral RNA was extracted from 200µL
501 using a QiaCube automated platform according to the manufacturer's
502 instructions (Cador Pathogen QIAcube HT kit; Qiagen, Toronto, Canada).
503 Allantoic fluids from *in ovo* experiments were collected and viral RNA was
504 extracted from 140µL according to the manufacturer's instructions

505 (QIAamp viral RNA; Qiagen, Toronto, Canada). cDNA was synthesized by
506 reverse transcription of 5µL of RNA, using a HA-specific primer (5'-
507 GTCCTTGCGACTG-3') and a RevertAid first-strand cDNA synthesis kit
508 (Invitrogen, Thermo Fisher Scientific) according to the manufacturer's
509 instructions. Influenza nucleic acid load was determined by qPCR using
510 primers targeting either the polybasic or the monobasic HA cleavage site.
511 qPCR was performed in 384-well plates in a final volume of 10µL using a
512 Bravo automated liquid handling platform (Agilent Technologies, Palo Alto,
513 CA) and a ViaaA 7 real-time PCR system (Applied Biosystems, Foster City,
514 CA) at the GeT-TRiX platform (GénoToul, Génopole, Toulouse, France).
515 Mixes were prepared according to the manufacturer's instructions (iTaq
516 SYBR green PCR, BioRad) with 2µL of cDNA and a final concentration of
517 0.5µM of each primer. Absolute quantification was performed using a
518 standard curve based on 10-fold serial dilutions of plasmid containing
519 either $H5N8_{LP}$ or $H5N8_{HP}$ HA gene.
520
521 **RNA extraction from tissue samples and cDNA synthesis**
522 For each organ, 30mg portions of tissue were placed in tubes with beads
523 (Precellys lysis kit; Stretton Scientific, Ltd., Stretton, United Kingdom) filled
524 with 1mL of TRIzol reagent (Invitrogen, Carlsbad, CA) and mixed for 5s at
525 6,000rpm three times in a bead beater (Precellys 24; Bertin Technologies,
526 Montigny-le-Bretonneux, France). After TRIzol extraction, the aqueous
527 phase was transferred to a RNA extraction column and processed according
528 to the manufacturer's instructions (NucleoSpin RNA; Macherey-Nagel
529 GmbH & Co, Germany). cDNA was synthesized by reverse transcription of
530 500ng of total RNA using either both oligo(dT)18 (0.25µg) and random
531 hexamer (0.1µg) primers or HA-specific primer and a RevertAid first-
532 strand cDNA synthesis kit (Invitrogen, Thermo Fisher Scientific) according
533 to the manufacturer's instructions.
534
535 **Quantitative PCR from tissue samples**
536 Quantitative PCR for the analysis of host genes expression was performed
537 in 384-well plates in a final volume of 10µL using a Bravo automated liquid

538 handling platform (Agilent Technologies, Palo Alto, CA) and a ViiA 7 real-
539 time PCR system (Applied Biosystems, Foster City, CA) at the GeT-TRiX
540 platform (GenoToul, Genopole, Toulouse, France). Mixes were prepared
541 according to the manufacturer's instructions (iTaq SYBR green PCR,
542 BioRad) with 2µl of 1:20 diluted cDNA and a final 0.5µM concentration of
543 each primer (Table 1). Quantification of influenza virus nucleic acid load in
544 tissues was performed in 96-well plates with a 10µL final volume according
545 to the manufacturer's instructions (iTaq SYBR green PCR, BioRad), along
546 with 2µL of cDNA and a final 0.5µM concentration of $H5N8_{HP}$ or $H5N8_{LP}$
547 specific primers. qPCR was performed on a LightCycler 96 (Roche). Relative
548 quantification was carried out by using the $2^{-\Delta Ct}$ method. Chickens: RNA
549 levels were normalized with the geometric mean of GAPDH/HPRT1 mRNA
550 levels. Ducks: mRNA levels were normalized with the geometrics means of
551 RPL4/RPL30 mRNA levels in the lungs and RPL4/GAPDH in the brain.
552 Oropharyngeal Mx mRNA expression was performed in 96-well plates with
553 a final volume of 10µL according to the manufacturer's instructions (iTaq
554 SYBR green one-step, BioRad), with 2µL RNA and a final 0.3µM
555 concentration of each primer. Mx mRNA levels were normalized with
556 GAPDH mRNA levels in chickens and ducks samples using the $2^{-\Delta Ct}$ method.
557
558 **Immunohistochemistry**
559 Tissue samples of the lungs and brain were taken and stored in 10%
560 neutral formalin. After fixation, tissues were processed in paraffin blocks,
561 sectioned at 4µm, and immunohistochemistry was performed on paraffin-
562 embedded sections with a monoclonal mouse anti-nucleoprotein influenza
563 A virus antibody (Argene 11-030; pronase 0.05% retrieval solution, 10 min
564 at 37°C: antibody dilution 1/50, incubation overnight at 4°C). The
565 immunohistochemical staining was revealed with a biotinylated polyclonal
566 goat anti-mouse immunoglobulin conjugated with horseradish peroxidase
567 (HRP; Dako, LSAB2 system-HRP, K0675) and the diaminobenzidine HRP
568 chromogen (Thermo Scientific, TA-125-HDX). Negative controls comprised
569 sections incubated either without specific primary antibody or with
570 another monoclonal antibody of the same isotype (IgG2).

571

572 Table 1: Primers used for qPCR

Gene name	Primers sequences (5' to 3')	NCBI accession number or Reference
HA $H5N8_{HP}$	CCCAAACAGCCCTCTTT	
	GGCTCAGAAATAGTCCTCT	
HA $H5N8_{LP}$	GCCATTCATCCACAGTTGACA	
	CATGGTGCTGACAGTGGAGTCT	
HA $H5N8_{LP}$ and $_{HP}$	GACCTCTGTTACCCAGGGAGCCT	
	GGACAAGCTGCGCTTACCCCT	
Chicken HPRT1	TGGTGGGGATGACCTCTCAA	(Garrido et al., 2017)
	GGCCGATATCCCACACTTCG	
Chicken GADPH	TCCTCTCTGGCAAAGTCCAAG	(Figueroa et al., 2016)
	CACAACATACTCAGCACCTGC	
Duck GAPDH	CCACTTCCGGGGCACTGTCA	AY436595.1
	AGCACCAGCATCTGCCCACT	
Chicken IFN-γ	ACACTGACAAGTCAAAGCCGC	(Brisbin et al., 2010)
	AGTCGTTCATCGGGAGCTTG	
Duck IFN-γ	ACCTCGTGGAACTGTCAAACCT	AF087134
	CAGCTCACTCACAGCCTTGC	
Chicken Mx	CACTGCAACAAGCAAAGAAGGA	(James et al., 2019)
	TGATCAACCCCACAAGGAAAA	
Duck Mx	TCACACGAAGGCCTATTTTACTGG	Z21549
	GTCGCCGAAGTCATGAAGGA	
Duck RPL4	AAGCTGAACCCATACGCCAA	XM_005015528
	CCTGGGCCTTAGCTGTAACC	

Duck RPL30	GCAAAGCCAAGCTGGTCATC	XM_027452502.1
	CTCAATGTTGTTGCCGCTGT	

573 GAPDH, glyceraldehyde-3-phosphate dehydrogenase; HPRT1, hypoxanthine
574 phosphoribosyltransferase 1; IFN-γ, interferon gamma; Mx, Mx Dynamin Like
575 GTPase; RPL4/30, ribosomal protein L4/L30; F, forward; R, reverse
576

577 ## REFERENCES

578

579 Abdelwhab E-SM, Veits J, Mettenleiter TC. 2013. Genetic changes that accompanied shifts of
580 low pathogenic avian influenza viruses toward higher pathogenicity in poultry.
581 *Virulence* **4**:441–452. doi:10.4161/viru.25710
582 Andreu-Moreno I, Bou J-V, Sanjuán R. 2020. Cooperative nature of viral replication. *Sci Adv*
583 **6**. doi:10.1126/sciadv.abd4942
584 Baccam P, Beauchemin C, Macken CA, Hayden FG, Perelson AS. 2006. Kinetics of Influenza A
585 Virus Infection in Humans. *Journal of Virology* **80**:7590–7599.
586 doi:10.1128/JVI.01623-05
587 Barber MRW, Aldridge JR, Webster RG, Magor KE. 2010. Association of RIG-I with innate
588 immunity of ducks to influenza. *Proc Natl Acad Sci USA* **107**:5913–5918.
589 doi:10.1073/pnas.1001755107
590 Bodewes R, Kuiken T. 2018. Changing Role of Wild Birds in the Epidemiology of Avian
591 Influenza A Viruses. *Adv Virus Res* **100**:279–307. doi:10.1016/bs.aivir.2017.10.007
592 Böttcher-Friebertshäuser E, Garten W, Matrosovich M, Klenk HD. 2014. The Hemagglutinin:
593 A Determinant of Pathogenicity In: Compans RW, Oldstone MBA, editors. Influenza
594 Pathogenesis and Control - Volume I, Current Topics in Microbiology and
595 Immunology. Cham: Springer International Publishing. pp. 3–34.
596 doi:10.1007/82_2014_384
597 Bou J-V, Geller R, Sanjuán R. 2019. Membrane-Associated Enteroviruses Undergo
598 Intercellular Transmission as Pools of Sibling Viral Genomes. *Cell Rep* **29**:714-723.e4.
599 doi:10.1016/j.celrep.2019.09.014
600 Brisbin JT, Gong J, Parvizi P, Sharif S. 2010. Effects of lactobacilli on cytokine expression by
601 chicken spleen and cecal tonsil cells. *Clin Vaccine Immunol* **17**:1337–1343.
602 doi:10.1128/CVI.00143-10
603 Brooke CB. 2017. Population Diversity and Collective Interactions during Influenza Virus
604 Infection. *Journal of Virology* **91**. doi:10.1128/JVI.01164-17
605 Burggraaf S, Karpala AJ, Bingham J, Lowther S, Selleck P, Kimpton W, Bean AGD. 2014. H5N1
606 infection causes rapid mortality and high cytokine levels in chickens compared to
607 ducks. *Virus Res* **185**:23–31. doi:10.1016/j.virusres.2014.03.012
608 Capua I, Marangon S. 2000. The avian influenza epidemic in Italy, 1999-2000: a review. *Avian*
609 *Pathol* **29**:289–294. doi:10.1080/03079450050118403
610 Cornelissen JBWJ, Post J, Peeters B, Vervelde L, Rebel JMJ. 2012. Differential innate
611 responses of chickens and ducks to low-pathogenic avian influenza. *Avian Pathol*
612 **41**:519–529. doi:10.1080/03079457.2012.732691
613 Cornelissen JBWJ, Vervelde L, Post J, Rebel JMJ. 2013. Differences in highly pathogenic avian
614 influenza viral pathogenesis and associated early inflammatory response in chickens
615 and ducks. *Avian Pathol* **42**:347–364. doi:10.1080/03079457.2013.807325
616 DaPalma T, Doonan BP, Trager NM, Kasman LM. 2010. A systematic approach to virus–virus
617 interactions. *Virus Research* **149**:1–9. doi:10.1016/j.virusres.2010.01.002
618 Dhingra MS, Artois J, Dellicour S, Lemey P, Dauphin G, Von Dobschuetz S, Van Boeckel TP,
619 Castellan DM, Morzaria S, Gilbert M. 2018. Geographical and Historical Patterns in
620 the Emergences of Novel Highly Pathogenic Avian Influenza (HPAI) H5 and H7
621 Viruses in Poultry. *Front Vet Sci* **5**. doi:10.3389/fvets.2018.00084
622 Domingo-Calap P, Segredo-Otero E, Durán-Moreno M, Sanjuán R. 2019. Social evolution of
623 innate immunity evasion in a virus. *Nat Microbiol* **4**:1006–1013. doi:10.1038/s41564-
624 019-0379-8

625 EFSA Panel on Animal Health and Welfare (AHAW), More S, Bicout D, Bøtner A, Butterworth
626 A, Calistri P, Depner K, Edwards S, Garin-Bastuji B, Good M, Gortázar Schmidt C,
627 Michel V, Miranda MA, Nielsen SS, Raj M, Sihvonen L, Spoolder H, Thulke H-H,
628 Velarde A, Willeberg P, Winckler C, Breed A, Brouwer A, Guillemain M, Harder T,
629 Monne I, Roberts H, Baldinelli F, Barrucci F, Fabris C, Martino L, Mosbach-Schulz O,
630 Verdonck F, Morgado J, Stegeman JA. 2017. Avian influenza. *EFSA J* **15**:e04991.
631 doi:10.2903/j.efsa.2017.4991
632 Farci P, Strazzera R, Alter HJ, Farci S, Degioannis D, Coiana A, Peddis G, Usai F, Serra G,
633 Chessa L, Diaz G, Balestrieri A, Purcell RH. 2002. Early changes in hepatitis C viral
634 quasispecies during interferon therapy predict the therapeutic outcome. *Proc Natl*
635 *Acad Sci U S A* **99**:3081–3086. doi:10.1073/pnas.052712599
636 Figueroa T, Bessière P, Coggon A, Bouwman KM, van der Woude R, Delverdier M, Verheije
637 MH, de Vries RP, Volmer R. 2020. The Microbiota Contributes to the Control of
638 Highly Pathogenic H5N9 Influenza Virus Replication in Ducks. *J Virol* **94**.
639 doi:10.1128/JVI.00289-20
640 Figueroa T, Boumart I, Coupeau D, Rasschaert D. 2016. Hyperediting by ADAR1 of a new
641 herpesvirus lncRNA during the lytic phase of the oncogenic Marek's disease virus.
642 *Journal of General Virology,* **97**:2973–2988. doi:10.1099/jgv.0.000606
643 Garrido D, Chanteloup NK, Trotereau A, Lion A, Bailleul G, Esnault E, Trapp S, Quéré P,
644 Schouler C, Guabiraba R. 2017. Characterization of the Phospholipid Platelet-
645 Activating Factor As a Mediator of Inflammation in Chickens. *Front Vet Sci* **4**.
646 doi:10.3389/fvets.2017.00226
647 Graaf A, Ulrich R, Maksimov P, Scheibner D, Koethe S, Abdelwhab EM, Mettenleiter TC, Beer
648 M, Harder T. 2018. A viral race for primacy: co-infection of a natural pair of low and
649 highly pathogenic H7N7 avian influenza viruses in chickens and embryonated
650 chicken eggs. *Emerg Microbes Infect* **7**:204. doi:10.1038/s41426-018-0204-0
651 Grund C, Hoffmann D, Ulrich R, Naguib M, Schinköthe J, Hoffmann B, Harder T, Saenger S,
652 Zscheppang K, Tönnies M, Hippenstiel S, Hocke A, Wolff T, Beer M. 2018. A novel
653 European H5N8 influenza A virus has increased virulence in ducks but low zoonotic
654 potential. *Emerg Microbes Infect* **7**:132. doi:10.1038/s41426-018-0130-1
655 Guinat C, Nicolas G, Vergne T, Bronner A, Durand B, Courcoul A, Gilbert M, Guérin J-L, Paul
656 MC. 2018. Spatio-temporal patterns of highly pathogenic avian influenza virus
657 subtype H5N8 spread, France, 2016 to 2017. *Eurosurveillance* **23**:1700791.
658 doi:10.2807/1560-7917.ES.2018.23.26.1700791
659 Hagenaars TJ, Fischer E a. J, Jansen CA, Rebel JMJ, Spekreijse D, Vervelde L, Backer JA, Jong
660 MCM de, Koets AP. 2016. Modelling the Innate Immune Response against Avian
661 Influenza Virus in Chicken. *PLOS ONE* **11**:e0157816.
662 doi:10.1371/journal.pone.0157816
663 Hiono T, Okamatsu M, Igarashi M, McBride R, de Vries RP, Peng W, Paulson JC, Sakoda Y,
664 Kida H. 2016. Amino acid residues at positions 222 and 227 of the hemagglutinin
665 together with the neuraminidase determine binding of H5 avian influenza viruses to
666 sialyl Lewis X. *Arch Virol* **161**:307–316. doi:10.1007/s00705-015-2660-3
667 Hoffmann E, Neumann G, Kawaoka Y, Hobom G, Webster RG. 2000. A DNA transfection
668 system for generation of influenza A virus from eight plasmids. *Proc Natl Acad Sci*
669 *USA* **97**:6108–6113. doi:10.1073/pnas.100133697
670 Hoffmann E, Stech J, Guan Y, Webster RG, Perez DR. 2001. Universal primer set for the full-
671 length amplification of all influenza A viruses. *Arch Virol* **146**:2275–2289.
672 Holzinger D, Jorns C, Stertz S, Boisson-Dupuis S, Thimme R, Weidmann M, Casanova J-L,
673 Haller O, Kochs G. 2007. Induction of MxA Gene Expression by Influenza A Virus
674 Requires Type I or Type III Interferon Signaling. *Journal of Virology* **81**:7776–7785.
675 doi:10.1128/JVI.00546-06

676 Honce R, Karlsson EA, Wohlgemuth N, Estrada LD, Meliopoulos VA, Yao J, Schultz-Cherry S.
677 2020. Obesity-Related Microenvironment Promotes Emergence of Virulent Influenza
678 Virus Strains. *mBio* **11**. doi:10.1128/mBio.03341-19
679 Hughes J, Allen RC, Baguelin M, Hampson K, Baillie GJ, Elton D, Newton JR, Kellam P, Wood
680 JLN, Holmes EC, Murcia PR. 2012. Transmission of Equine Influenza Virus during an
681 Outbreak Is Characterized by Frequent Mixed Infections and Loose Transmission
682 Bottlenecks. *PLOS Pathogens* **8**:e1003081. doi:10.1371/journal.ppat.1003081
683 James J, Smith N, Ross C, Iqbal M, Goodbourn S, Digard P, Barclay WS, Shelton H. 2019. The
684 cellular localization of avian influenza virus PB1-F2 protein alters the magnitude of
685 IFN2 promoter and NFκB-dependent promoter antagonism in chicken cells. *Journal*
686 *of General Virology,* **100**:414–430. doi:10.1099/jgv.0.001220
687 Kleyheeg E, Slaterus R, Bodewes R, Rijks JM, Spierenburg MAH, Beerens N, Kelder L, Poen
688 MJ, Stegeman JA, Fouchier RAM, Kuiken T, van der Jeugd HP. 2017. Deaths among
689 Wild Birds during Highly Pathogenic Avian Influenza A(H5N8) Virus Outbreak, the
690 Netherlands. *Emerg Infect Dis* **23**:2050–2054. doi:10.3201/eid2312.171086
691 Kuchipudi SV, Tellabati M, Sebastian S, Londt BZ, Jansen C, Vervelde L, Brookes SM, Brown
692 IH, Dunham SP, Chang K-C. 2014. Highly pathogenic avian influenza virus infection in
693 chickens but not ducks is associated with elevated host immune and pro-
694 inflammatory responses. *Vet Res* **45**:118. doi:10.1186/s13567-014-0118-3
695 Kumar N, Sharma S, Barua S, Tripathi BN, Rouse BT. 2018. Virological and Immunological
696 Outcomes of Coinfections. *Clinical Microbiology Reviews* **31**.
697 doi:10.1128/CMR.00111-17
698 Kuss SK, Etheredge CA, Pfeiffer JK. 2008. Multiple host barriers restrict poliovirus trafficking
699 in mice. *PLoS Pathog* **4**:e1000082. doi:10.1371/journal.ppat.1000082
700 Lee D-H, Criado MF, Swayne DE. 2021. Pathobiological Origins and Evolutionary History of
701 Highly Pathogenic Avian Influenza Viruses. *Cold Spring Harb Perspect Med* **11**.
702 doi:10.1101/cshperspect.a038679
703 Leyson C, Youk S-S, Smith D, Dimitrov K, Lee D-H, Larsen LE, Swayne DE, Pantin-Jackwood
704 MJ. 2019. Pathogenicity and genomic changes of a 2016 European H5N8 highly
705 pathogenic avian influenza virus (clade 2.3.4.4) in experimentally infected mallards
706 and chickens. *Virology* **537**:172–185. doi:10.1016/j.virol.2019.08.020
707 Li S, Bai S, Qin X, Zhang J, Irwin DM, Zhang S, Wang Z. 2019. Comparison of whole embryonic
708 development in the duck (Anas platyrhynchos) and goose (Anser cygnoides) with the
709 chicken (Gallus gallus). *Poultry Science* **98**:3278–3291. doi:10.3382/ps/pez133
710 Magor KE, Miranzo Navarro D, Barber MRW, Petkau K, Fleming-Canepa X, Blyth GAD, Blaine
711 AH. 2013. Defense genes missing from the flight division. *Developmental &*
712 *Comparative Immunology*, Chicken Immunity **41**:377–388.
713 doi:10.1016/j.dci.2013.04.010
714 M.c JD, A S, Der GJV, G K. 2009. Intra- and interspecies transmission of H7N7 highly
715 pathogenic avian influenza virus during the avian influenza epidemic in the
716 Netherlands in 2003 **28**:333–340. doi:10.20506/rst.28.1.1859
717 McCrone JT, Lauring AS. 2018. Genetic bottlenecks in intraspecies virus transmission. *Current*
718 *Opinion in Virology*, Emerging viruses: intraspecies transmission • Viral Immunology
719 **28**:20–25. doi:10.1016/j.coviro.2017.10.008
720 More S, Bicout D, Bøtner A, Butterworth A, Calistri P, Depner K, Edwards S, Garin-Bastuji B,
721 Good M, Schmidt CG, Michel V, Miranda MA, Nielsen SS, Raj M, Sihvonen L, Spoolder
722 H, Thulke HH, Velarde A, Willeberg P, Winckler C, Adlhoch C, Baldinelli F, Breed A,
723 Brouwer A, Guillemain M, Harder T, Monne I, Roberts H, Abrahantes JC, Mosbach-
724 Schulz O, Verdonck F, Morgado J, Stegeman A. 2017. Urgent request on avian
725 influenza. *EFSA Journal* **15**:e04687. doi:https://doi.org/10.2903/j.efsa.2016.4687

726 Munster VJ, Baas C, Lexmond P, Waldenström J, Wallensten A, Fransson T, Rimmelzwaan GF,
727 Beyer WEP, Schutten M, Olsen B, Osterhaus ADME, Fouchier RAM. 2007. Spatial,
728 Temporal, and Species Variation in Prevalence of Influenza A Viruses in Wild
729 Migratory Birds. *PLOS Pathog* **3**:e61. doi:10.1371/journal.ppat.0030061
730 Opatowski L, Baguelin M, Eggo RM. 2018. Influenza interaction with cocirculating pathogens
731 and its impact on surveillance, pathogenesis, and epidemic profile: A key role for
732 mathematical modelling. *PLOS Pathogens* **14**:e1006770.
733 doi:10.1371/journal.ppat.1006770
734 Organization WH. 2008. Addressing ethical issues in pandemic influenza planning: discussion
735 papers. World Health Organization.
736 Phipps KL, Ganti K, Jacobs NT, Lee C-Y, Carnaccini S, White MC, Manandhar M, Pickett BE,
737 Tan GS, Ferreri LM, Perez DR, Lowen AC. 2020. Collective interactions augment
738 influenza A virus replication in a host-dependent manner. *Nat Microbiol* **5**:1158–
739 1169. doi:10.1038/s41564-020-0749-2
740 Poultry species | Gateway to poultry production and products | Food and Agriculture
741 Organization of the United Nations. n.d. http://www.fao.org/poultry-production-
742 products/production/poultry-species/en/
743 Richard M, Fouchier R, Monne I, Kuiken T. 2017. Mechanisms and risk factors for mutation
744 from low to highly pathogenic avian influenza virus. *EFSA Supporting Publications*
745 **14**:1287E. doi:10.2903/sp.efsa.2017.EN-1287
746 Soubies SM, Hoffmann TW, Croville G, Larcher T, Ledevin M, Soubieux D, Quéré P, Guérin J-L,
747 Marc D, Volmer R. 2013. Deletion of the C-terminal ESEV domain of NS1 does not
748 affect the replication of a low-pathogenic avian influenza virus H7N1 in ducks and
749 chickens. *J Gen Virol* **94**:50–58. doi:10.1099/vir.0.045153-0
750 van Dijk JG, Verhagen JH, Wille M, Waldenström J. 2018. Host and virus ecology as
751 determinants of influenza A virus transmission in wild birds. *Curr Opin Virol* **28**:26–
752 36. doi:10.1016/j.coviro.2017.10.006
753 Varble A, Albrecht RA, Backes S, Crumiller M, Bouvier NM, Sachs D, García-Sastre A,
754 tenOever BR. 2014. Influenza A Virus Transmission Bottlenecks Are Defined by
755 Infection Route and Recipient Host. *Cell Host & Microbe* **16**:691–700.
756 doi:10.1016/j.chom.2014.09.020
757 Volmer C, Soubies SM, Grenier B, Guérin J-L, Volmer R. 2011. Immune response in the duck
758 intestine following infection with low-pathogenic avian influenza viruses or
759 stimulation with a Toll-like receptor 7 agonist administered orally. *J Gen Virol*
760 **92**:534–543. doi:10.1099/vir.0.026443-0
761 Wahlgren J. 2011. Influenza A viruses: an ecology review. *Infect Ecol Epidemiol* **1**.
762 doi:10.3402/iee.v1i0.6004
763 Zwart MP, Elena SF. 2015. Matters of Size: Genetic Bottlenecks in Virus Infection and Their
764 Potential Impact on Evolution. *Annu Rev Virol* **2**:161–179. doi:10.1146/annurev-
765 virology-100114-055135
766

767

768

769

770

ACKNOWLEDGEMENTS

This work was funded by a grant from the Agence Nationale de la Recherche (ANR-16-CE35-0005-01) to Romain Volmer. Pierre Bessière was supported by a Ph.D. scholarship funded by the Region Occitanie (France) and by the Chaire de Biosécurité at the École Nationale Vétérinaire de Toulouse (French Ministry of Agriculture). Maxime Fusade-Boyer and Gabriel Dupré are supported by PhD scholarships funded by the French Ministry of Research and Education.

AUTHOR CONTRIBUTIONS

Pierre Bessière, Conceptualization, Formal analysis, Investigation, Visualization, Methodology, Writing – original draft; Thomas Figueroa, Conceptualization, Formal analysis, Investigation, Visualization, Methodology, Writing – review and editing; Amelia Coggon, Charlotte Foret-Lucas, Alexandre Houffschmitt, Maxime Fusade-Boyer, Gabriel Dupré, Jean-Luc Guérin, Maxence Delverdier, Investigation, Writing – review and editing; Romain Volmer, Conceptualization, Formal analysis, Investigation, Visualization, Methodology, Funding acquisition, Writing – original draft, Writing – review and editing, Funding acquisition, Project administration.

COMPETING INTERESTS

The authors declare no competing interests.

ETHICS

This study was carried out in compliance with European animal welfare regulation. The protocols were approved by the Animal Care and Use Committee (Comité d'Ethique en Science et Santés Animales – 115) under protocol 13025-2018012311319709.

MATERIALS & CORRESPONDANCE

Correspondence and material requests should be addressed to Romain Volmer (romain.volmer@envt.fr).

FIGURES

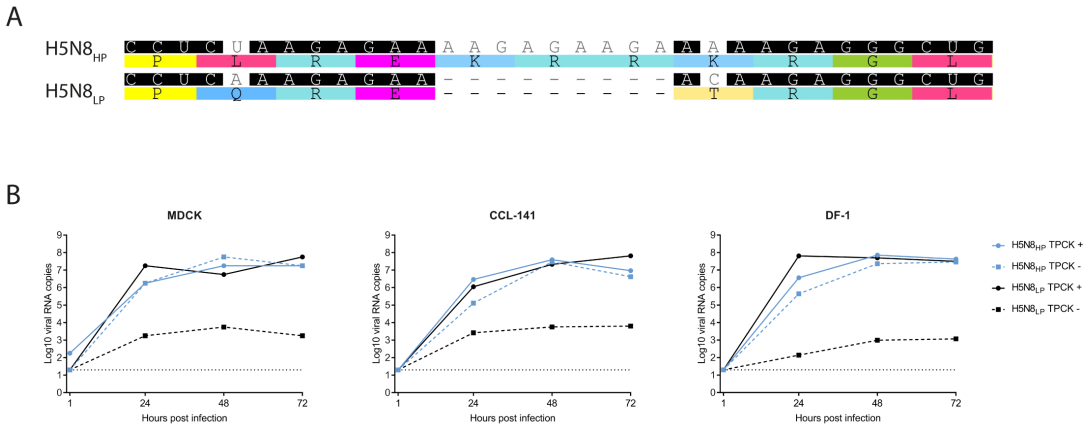

Fig. 1. Characterization of $H5N8_{HP}$ and $H5N8_{LP}$ viruses in cell culture. (A) Sequence alignment of $H5N8_{HP}$ and $H5N8_{LP}$ HA cleavage sites. **(B)** $H5N8_{HP}$ and $H5N8_{LP}$ growth kinetics in the absence or presence of exogenous trypsin in Madin-Darby canine kidney (MDCK) cells, DF-1 cells and CCL-141 cells. Cells were infected at a MOI of 10^{-5} $TCID_{50}$. HA RNA load was analyzed by RT-qPCR using primers common to $H5N8_{HP}$ and $H5N8_{LP}$. The dotted line represents the limit of detection for each experiment. Results are representative of an experiment performed three times.

A

	H2	L2H2	L3H2	L4H2	L5H2	L2	L3	L4	L5
$H5N8_{HP}$	10^2 EID_{50}	10^2 EID_{50}	10^2 EID_{50}	10^2 EID_{50}	10^4 EID_{50}	-	-	-	-
$H5N8_{LP}$	-	10^2 EID_{50}	10^3 EID_{50}	10^4 EID_{50}	10^5 EID_{50}	10^2 EID_{50}	10^3 EID_{50}	10^4 EID_{50}	10^5 EID_{50}

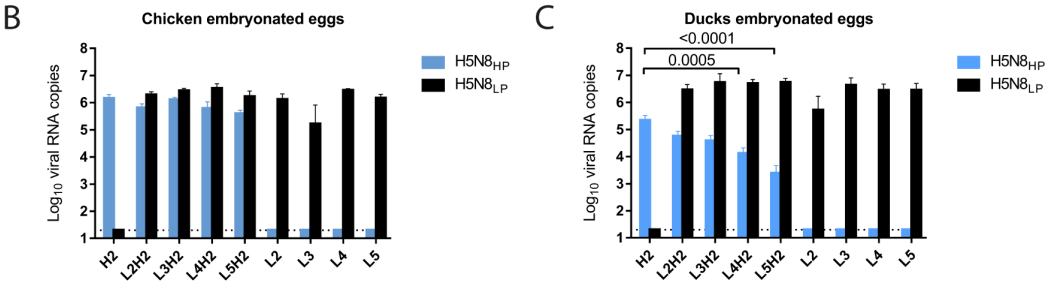

Fig. 2. $H5N8_{HP}$ has a stronger advantage over $H5N8_{LP}$ in embryonated chicken eggs than in embryonated duck eggs. (A) EID_{50} doses used in the *in ovo* experiments**. (B-C)** Chicken **(B)** and duck **(C)** embryonated eggs were infected in the allantoic cavity either with $H5N8_{HP}$ or $H5N8_{LP}$ alone, or with a combination of both. Following a 24 hours incubation at 37°C, viral RNA was extracted from the allantoic fluid and HA levels were determined by RT-qPCR using $H5N8_{HP}$ or $H5N8_{LP}$ specific primers. Statistical analysis: chicken embryonated eggs: n=9 (experiment performed twice); duck embryonated eggs: n=26 (experiment performed three times); one-way ANOVA with Tukey's multiple comparisons test. Results are expressed as means ± SEM. The dotted line represents the limit of detection for each experiment.

807

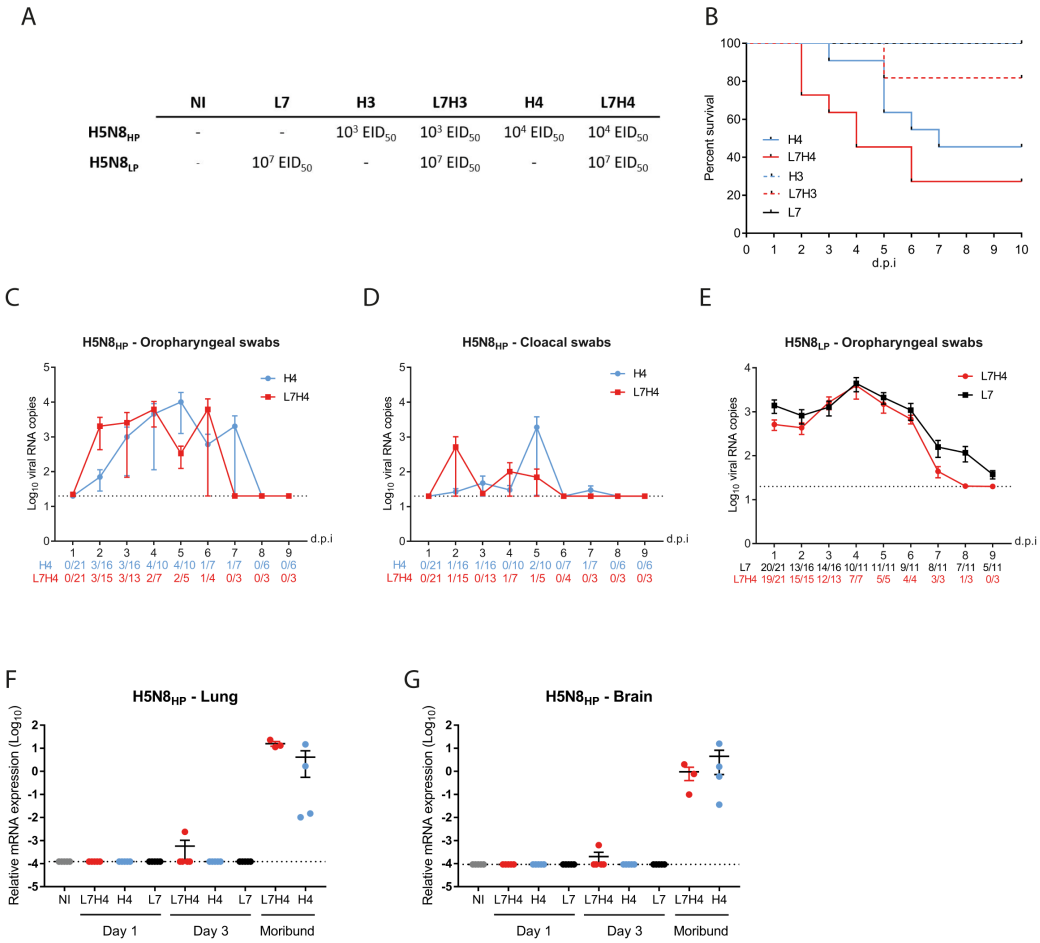

Fig. 3. H5N8$_{HP}$ and H5N8$_{LP}$ coinfection in chickens results in increased pathogenesis. Chickens were inoculated via the choanal route with H5N8$_{LP}$ alone (L7), H5N8$_{HP}$ alone (H3 and H4) or with a combination of H5N8$_{LP}$ and H5N8$_{HP}$ (L7H3 and L7H4). **(A)** EID$_{50}$ doses used in the *in vivo* chicken experiments**. (B)** Survival curves. Statistical analysis: Log-rank (Mantel-Cox) test. **(C-E)** Viral shedding was analyzed by quantifying HA RNA levels by RT-qPCR using H5N8$_{HP}$ specific primers from RNA extracted from oropharyngeal swabs **(C)** and cloacal swabs **(D)** or by RT-qPCR using H5N8$_{LP}$ specific primers from RNA extracted from oropharyngeal swabs **(E)**. Numbers of H5N8$_{HP}$ or H5N8$_{HP}$ swab-positive animals are indicated below each time point. Statistical analysis: two-tailed Mann-Whitney test. Results are expressed as means ± SEM. The dotted line represents the limit of detection. **(F-G)** H5N8$_{HP}$ load was analyzed from total RNA extracted from the lungs **(F)** and the brain **(G)** using H5N8$_{HP}$ specific primers. HA RNA levels were normalized using the $2^{-\Delta Ct}$ method. Statistical analysis: one-way ANOVA with Tukey's multiple comparisons test. Results are expressed as means ± SEM. The dotted line represents the limit of detection. dpi, days post-infection.

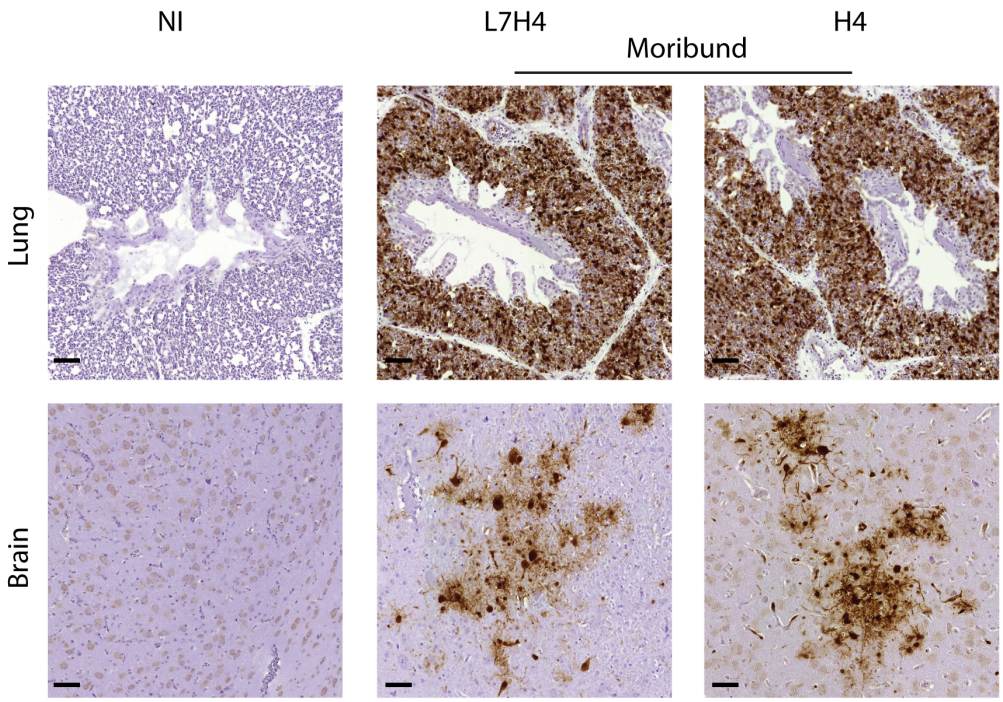

Fig. 4. Immunohistochemical anti-NP staining of hematoxylin-counterstained chickens lung or brain sections. Analysis was performed on non-infected (NI) and moribund chickens. Scale bar, 50 µm.

809

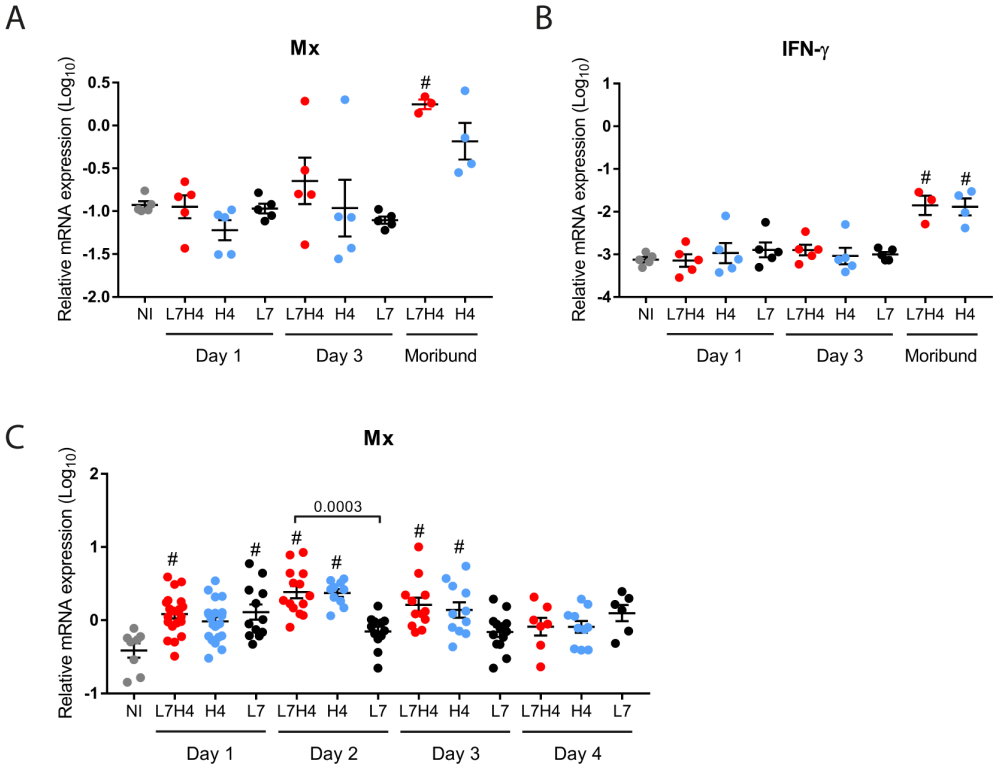

Fig. 5. Mx and IFN-γ mRNA expression following chickens infection. (A-B) mRNA expression levels of Mx **(A)** and IFN-γ **(B)** determined by RT-qPCR performed on lung total RNA. **(C)** mRNA expression levels of Mx determined by RT-qPCR performed on RNA extracted from oropharyngeal swabs. mRNA levels were normalized using the $2^{-\Delta Ct}$ method. Statistical analysis: one-way ANOVA with Tukey's multiple comparisons test. Results are expressed as means ± SEM. #, $p < 0.05$ compared to non-infected (NI) animals.

810

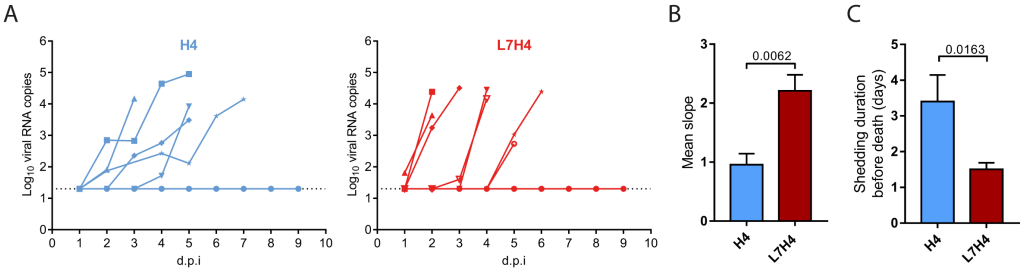

Fig. 6. H5N8$_{HP}$ and H5N8$_{LP}$ coinfection in chickens results in higher H5N8$_{HP}$ growth. (A) Individual H5N8$_{HP}$ oropharyngeal shedding curves in H4 chickens (blue lines) and L7H4 chickens (red lines). Each curve corresponds to a single animal from the onset of H5N8$_{HP}$ excretion to death. **(B)** The slopes of individual H5N8$_{HP}$ excretion curves were calculated. **(C)** H5N8$_{HP}$ shedding duration: number of days where chickens were H5N8$_{HP}$ oropharyngeal swab-positive. Statistical analysis: two-tailed Mann-Whitney test. Results are expressed as means ± SEM. The dotted line corresponds to the limit of detection. dpi, days post-infection.

811

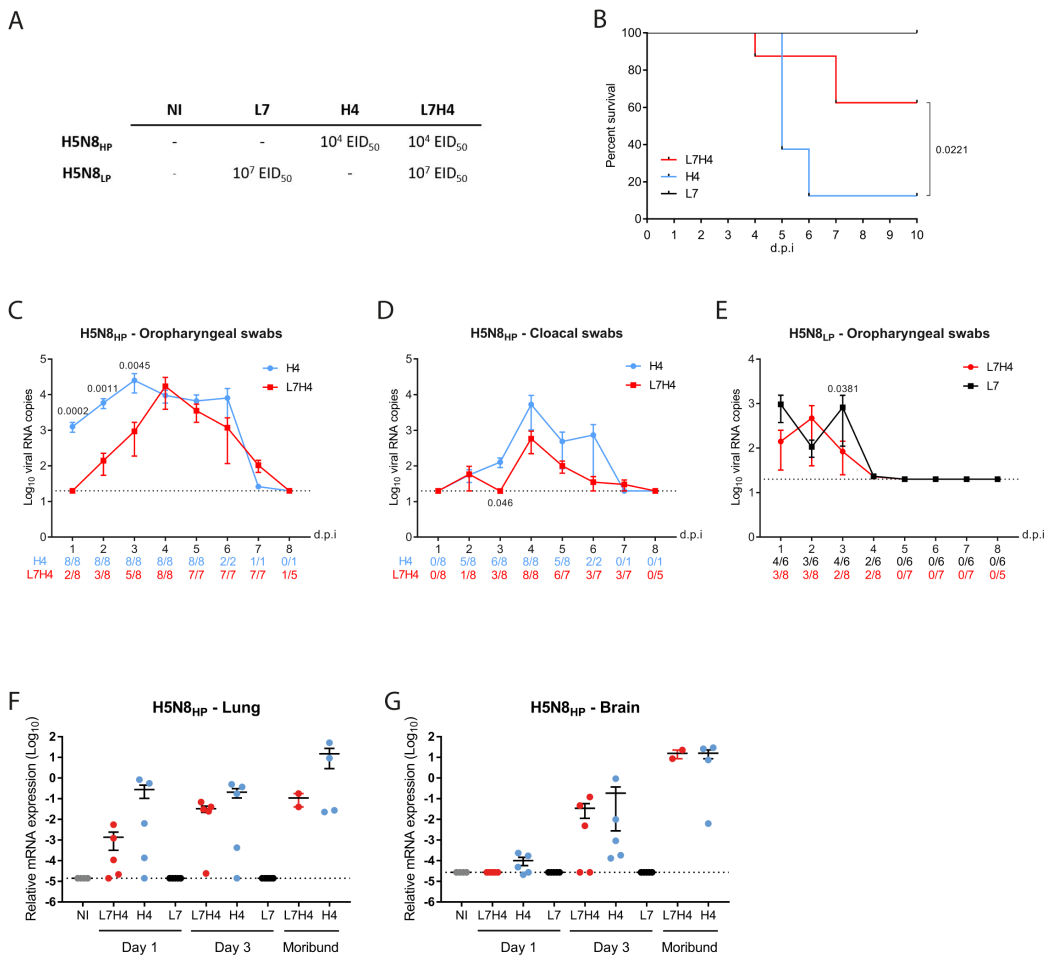

Fig. 7. H5N8$_{HP}$ and H5N8$_{LP}$ coinfection in ducks results in decreased pathogenesis. Ducks were inoculated via the choanal route with H5N8$_{LP}$ alone (L7), H5N8$_{HP}$ alone (H4) or with a combination of H5N8$_{LP}$ and H5N8$_{HP}$ (L7H4). **(A)** EID$_{50}$ doses used in the *in vivo* duck experiments**. (B)** Survival curves. Statistical analysis: Log-rank (Mantel-Cox) test. **(C-E)** Viral shedding was analyzed by quantifying HA RNA levels by RT-qPCR using H5N8$_{HP}$ specific primers from RNA extracted from oropharyngeal swabs **(C)** and cloacal swabs **(D)** or by RT-qPCR using H5N8$_{LP}$ specific primers from RNA extracted from oropharyngeal swabs **(E)**. Numbers of H5N8$_{HP}$ or H5N8$_{HP}$ swab-positive animals are indicated below each time point. Statistical analysis: two-tailed Mann-Whitney test. Results are expressed as means ± SEM. The dotted line represents the limit of detection. **(F-G)** H5N8$_{HP}$ load was analyzed from total RNA extracted from the lungs **(F)** and the brain **(G)** using H5N8$_{HP}$ specific primers. HA RNA levels were normalized using the $2^{-\Delta Ct}$ method. Statistical analysis: one-way ANOVA with Tukey's multiple comparisons test. Results are expressed as means ± SEM. The dotted line represents the limit of detection. dpi, days post-infection.

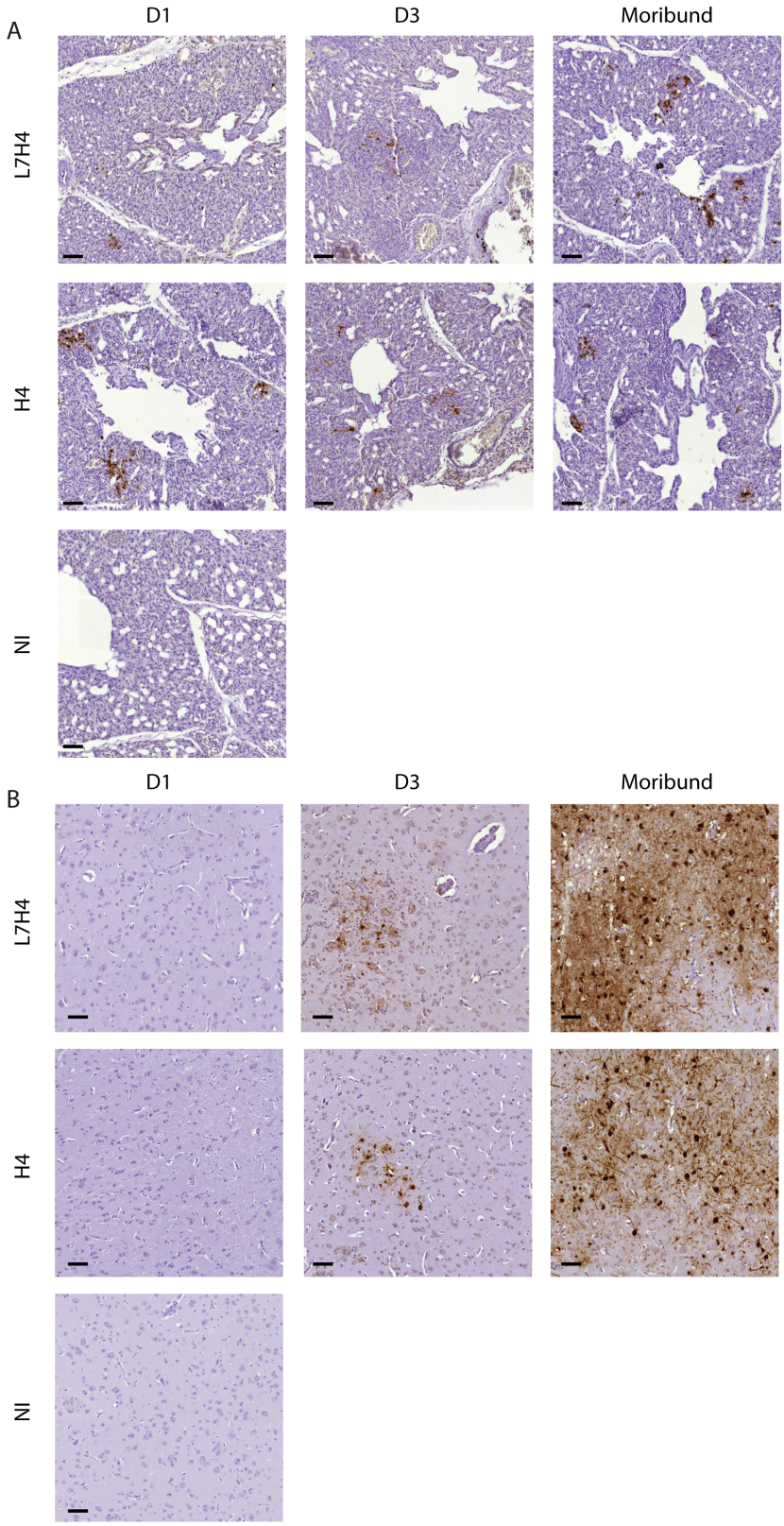

Fig. 8. Immunohistochemical anti-NP staining of hematoxylin-counterstained ducks lung or brain sections. Analysis was performed on ducks necropsied at 1 (D1) and 3 days (D3) post infection, moribund ducks and non-infected (NI) ducks. **(A)** Lung**. (B)** Brain. Scale bar, 50 µm.

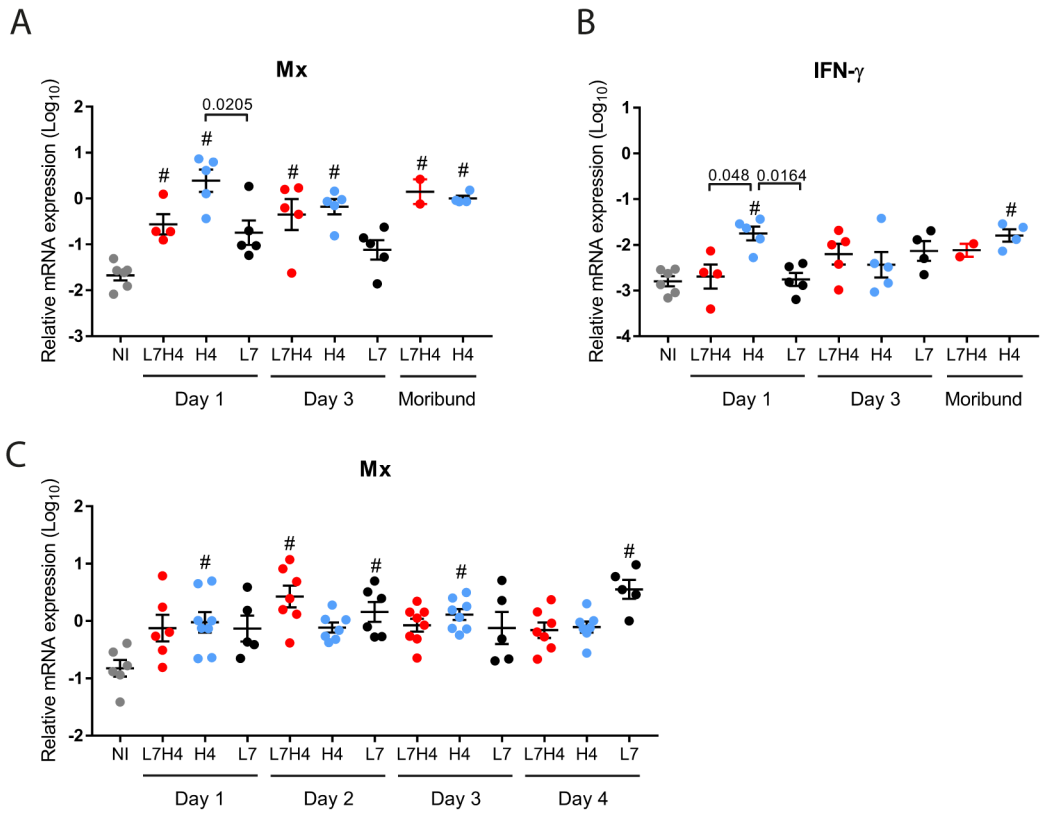

Fig. 9. Mx and IFN-γ mRNA expression following infection in ducks. (A-B) mRNA expression levels of Mx **(A)** and IFN-γ **(B)** determined by RT-qPCR performed on lung total RNA. **(C)** mRNA expression levels of Mx determined by RT-qPCR performed on RNA extracted from oropharyngeal swabs. mRNA levels were normalized using the $2^{-\Delta Ct}$ method. Statistical analysis: one-way ANOVA with Tukey's multiple comparisons test. Results are expressed as means ± SEM. #, $p < 0.05$ compared to non-infected (NI) animals.

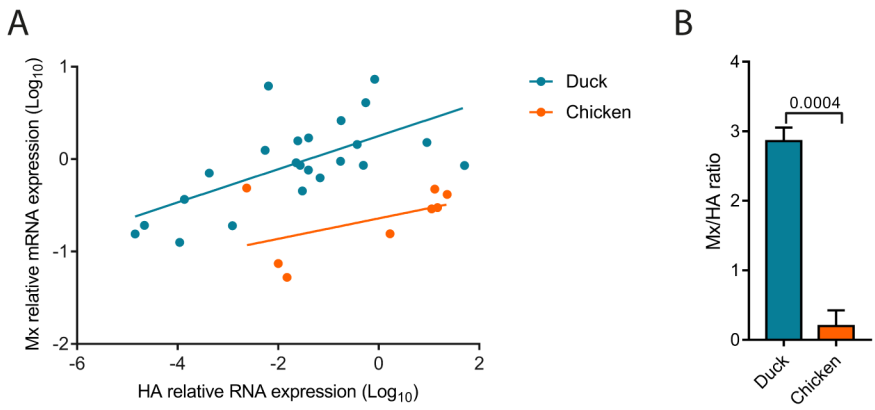

Fig. 10. Ducks mount a more potent antiviral innate immune response compared to chickens. (A) Correlation between Mx mRNA levels and viral RNA levels in the lungs. **(B)** Mean Mx/HA ratios. Mx mRNA and HA RNA levels were normalized using the $2^{-\Delta Ct}$ method. Statistical analysis: two-tailed Mann-Whitney test. Results are expressed as means ± SEM.

815

816